



HAL
open science

Nanomechanical and analytical investigations on tribological layers for wear protection in slow running roller bearings

Manuela Reichelt, Thomas Weirich, Silvia Richter, Anke Aretz, Matthias Bueckins, Thomas Wolf, P. W. Gold, Joachim Mayer

► **To cite this version:**

Manuela Reichelt, Thomas Weirich, Silvia Richter, Anke Aretz, Matthias Bueckins, et al.. Nanomechanical and analytical investigations on tribological layers for wear protection in slow running roller bearings. Philosophical Magazine, 2006, 86 (33-35), pp.5477-5495. 10.1080/14786430600786644 . hal-00513714

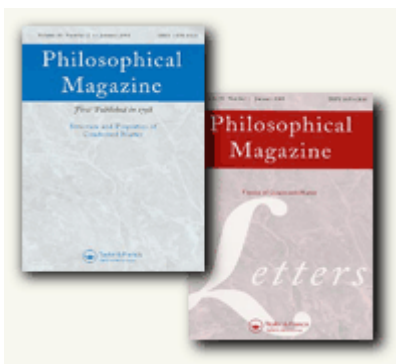
HAL Id: hal-00513714

<https://hal.science/hal-00513714>

Submitted on 1 Sep 2010

HAL is a multi-disciplinary open access archive for the deposit and dissemination of scientific research documents, whether they are published or not. The documents may come from teaching and research institutions in France or abroad, or from public or private research centers.

L'archive ouverte pluridisciplinaire **HAL**, est destinée au dépôt et à la diffusion de documents scientifiques de niveau recherche, publiés ou non, émanant des établissements d'enseignement et de recherche français ou étrangers, des laboratoires publics ou privés.



Nanomechanical and analytical investigations on tribological layers for wear protection in slow running roller bearings

Journal:	<i>Philosophical Magazine & Philosophical Magazine Letters</i>
Manuscript ID:	TPHM-05-Nov-0511.R2
Journal Selection:	Philosophical Magazine
Date Submitted by the Author:	23-Mar-2006
Complete List of Authors:	Reichelt, Manuela; RWTH Aachen University, Central Facility for Electron Microscopy Weirich, Thomas; RWTH Aachen University, Central Facility for Electron Microscopy Richter, Silvia; RWTH Aachen University, Central Facility for Electron Microscopy Aretz, Anke; RWTH Aachen University, Central Facility for Electron Microscopy Bueckins, Matthias; RWTH Aachen University, Central Facility for Electron Microscopy Wolf, Thomas; RWTH Aachen University, Institut for Machine Elements and Machine Design Gold, P. W.; RWTH Aachen University, Institut for Machine Elements and Machine Design Mayer, Joachim; RWTH Aachen University, Central Facility for Electron Microscopy
Keywords:	FIB, TEM, nanoindentation, tribology
Keywords (user supplied):	roller bearing, reaction layer

1
2
3
4
5
6
7
8
9
10
11
12
13
14
15
16
17
18
19
20
21
22
23
24
25
26
27
28
29
30
31
32
33
34
35
36
37
38
39
40
41
42
43
44
45
46
47
48
49
50
51
52
53
54
55
56
57
58
59
60



For Peer Review Only

Nanomechanical and analytical investigations on tribological layers for wear protection in slow running roller bearings

M. Reichelt[†], Th. Weirich[†], S. Richter[†], A. Aretz[†], M. Bückins[†], Th. Wolf[‡], P. W. Gold[‡] and J. Mayer[†]

[†] Central Facility for Electron Microscopy, RWTH Aachen University, Ahornstrasse 55, 52074 Aachen, Germany

[‡] Institut for Machine Elements and Machine Design, RWTH Aachen University, Schinkelstrasse 10, 52062 Aachen, Germany

reichelt@gfe.rwth-aachen.de

Keywords: reaction layer, roller bearing, nanoindentation, FIB, TEM, tribology

Abstract

In a tribological system consisting of roller thrust bearings and various lubricants, we investigated reaction layers formed under the presence of lubricants with low wear protection, high wear and fatigue protection as well as high wear but low fatigue protection. The bearings were tested under heavy-duty conditions in a FE-8 test rig in order to assess rapidly the efficiency of different reaction layer-systems. Chemical composition and microstructure analysis of the layers was subsequently carried out by transmission electron microscopy on thin cross sections prepared by the focused ion beam technique. The nanomechanical properties of the different tribological layers were analysed by nanoindentation. The formation and structure of the layered system, and thus the ability to protect against wear and fatigue, depends on the lubricants and additives, respectively. Our results indicate that wear protection not only relies on the reaction layer itself but also on the properties of the combined system of the reaction layer and an underlying tribomutation layer.

Introduction

Slow running roller bearings often suffer from the absence of a load-carrying hydrodynamical lubricating film. As a result, direct contacts of individual asperities can lead to highly localised energy dissipation with microplastic deformation and temperatures (hot spots) up to 700-800°C [1]. The occurrence of such hot spots leads to surface smoothing by filling existing valleys with sintered reaction products [2]. Another possible process is tribochemical erosion of asperities [1] or matrix amorphisation [2, 3]. In addition, there is evidence for the formation of an oxide layer in the rolling contact zone with a thickness in the range of $1 \dots 10^4$ nm. Evans et al. investigations on focused ion beam (FIB) cross-sectional lamella of surface - layers in sulphur-phosphorus (S-P) additive tribology revealed such oxide layers by transmission electron microscopy (TEM) analysis [4, 5]. Towards the underlying matrix, this reaction layer is followed by a tribomutation layer (thickness $< 10^4$ nm) which consists of a fine crystalline zone [2, 4, 5]. Based upon the present understanding, the composition and properties of the whole layer system depend strongly on the lubricant in use and in particular on the combination of additives [4, 5].

The aim of the present work is to verify the existence of reaction layers in the investigated model systems and to determine their chemical composition and microstructures by transmission electron microscopy (TEM) and electron probe micro analyser (EPMA) investigations and determine their micromechanical properties. The micromechanical properties were analysed by a statically depth-sensing nanoindentation device.

By combination of TEM analysis of Focused Ion Beam FIB cross-sectional lamella and nanoindentation measurements at load of 5000 μ N, we were able to perform a detailed investigation of the near surface properties. The samples for the present investigations were selected from different tribological systems, which consisted of axial cylindrical roller bearings tested in the presence of lubricants with low wear protection (mineral oil with Ca-P-S additives), high wear and fatigue protection (polyalphaolefine oil with ester and P-S additives), as well as high wear but low fatigue protection (mineral oil with Ca-Zn-P-S additives).

2 Experimental conditions

2.1 Tribological system

The investigations are based on wear experiments carried out under heavy-duty conditions in a standardised test rig for antifriction lubricant and bearing testing (FE-8, [6, 7]), in order to quickly distinguish the efficiency

of different reaction layer-systems. Axial cylinder roller thrust bearings (type 81212) consisting of 15 cylindrical rollers (100Cr6), a polyamid cage (Pa 66), a casing disc (100Cr6) and a shaft disc (100Cr6) under boundary lubrication condition were used. Due to the roller motion the axial cylinder roller bearing has a high slip contribution (maximum +/- 14.8%) and in addition the revolutions per minute is really slow 7,5 RPM. These resulted in a larger wear stress on the inner track than on the outer track of the bearing disc. In these conditions, the requirements on lubrication are very high [8].

The lubricants have been categorised according to the wear protection achieved during the standard tests on the FE-8 test rig. For the system with low wear protection, we used an ATF-oil based on mineral oil and Ca-P-S additives with a viscosity of 32 mm²/s at 40°C. An industrial gear oil based on polyalphaolefin (PAO/E)-oil and P-S additives with a viscosity of 100 mm²/s at 40°C was chosen for the bearing with high wear and fatigue protection. Lubrication with high wear but low fatigue protection was obtained by using a mineral oil with Ca-Zn-P-S additives and a viscosity of 98 mm²/s at 40°C, which is in common use as motor oil.

In the wear experiments, the load conditions were varied systematically at a temperature of 80°C by increasing or reducing the applied load in defined steps. The contact pressure was changed by increasing the normal force or by decreasing the numbers of rollers in the bearing. In this manner, five load levels were produced with contact pressure of 1150 MPa, 1490 MPa, 1890 MPa, 2300 MPa and 3250 MPa. The experiment always started with a standard condition, i. e. a normal force of 80 kN and 15 rollers, corresponding to a contact pressure of 1890 MPa. The bearings were tested at a load level which was one level below the load causing technical failure in order to determine the maximum load at which the reaction layer provides sufficient wear and fatigue protection. The wear criterion was evaluated by the gravimetric wear amount analysis. The mass loss of the fifteen rollers must be less than 10 mg after the wear experiment [9]. If a smaller number of rollers was used the mass loss is extrapolated to fifteen rollers.

2.2 Methods

The homogeneity, crystallinity and composition of the tribological layers is analysed by conventional transmission electron microscopy (TEM), high resolution TEM (HRTEM), selected area electron diffraction (SAED) and energy-filtering TEM (EFTEM) on a FEI Tecnai F20. The specimen preparation was performed on a Focused Ion Beam (FIB) workstation (FEI Strata FIB 205). The cross section investigations give detailed information on the formation of reaction layers and of tribomutation layers in the matrix. Micro-analytical characterization with an Electron Probe Micro Analyser (EPMA) instrument (Cameca, SX 50) makes it possible to determine the average oxygen coverage along line scans across the whole disc and to compute an average oxide thickness [10]. The spatially and depth resolved information on the surface roughness and micromechanical properties of the reaction layers, the tribomutation layers and the entire tribological system is determined by an add-on depth-sensing nanoindentation system (Hysitron TriboScope) attached to a commercial atomic force microscope (Park Scientific Instrument Autoprobe CP) [11]. The combination of a nanoindenter with an AFM has a symbiotic effect: it extends the AFM technique with the capability of making nanoindentation experiments with a load and depth resolution (100 nN and 0.2 nm, respectively). Thus the nanoindentation system can also be used to take scanning force images of the sample surface by scanning the same diamond tip across the sample surface.

2.3 Samples

Previous investigations revealed that the chemical and crystalline composition of the reference sample corresponds to the specification DIN EN ISO 683-17: 0.93-1.05 wt.% C, 0.15-0.35 wt.% Si, 0.25-0.45 wt.% Mn, 0.025 wt.% S, 1.35-1.60 wt.% Cr, max. 0.10 wt.% Mo and max. 0.050 wt.% Al [12]. All our present investigations were performed on one of the bearing discs of the tribological systems. The bearing with the lubricant with low wear protection was tested for 8 hours with contact pressure of 1150 MPa (load level one) and has already shown wear ($m > 10$ mg). The bearing with the lubricant with high wear and fatigue protection was tested for 80 hours with contact pressure of 2300 MPa (load level 4) and satisfied the wear criterion ($m < 10$ mg). The bearings with lubricant with high wear but low fatigue protection were tested for 80 hours at 3250 MPa ($m < 10$ mg), see table 1.

The sample preparation consisted in cutting the discs on a Vari/Cut V C-50 (Leco Corporation) low speed diamond saw in mineral spirit (Buehler) under water free conditions. The bearing discs were cut in small pieces suitable for further EPMA investigation, nanoindentation studies and TEM specimen preparation. EPMA-measurements show that the samples can be cleaned with acetone for 30 minutes in an ultrasonic bath without damaging the reaction layer.

The TEM specimen preparation was performed on a Focused Ion Beam (FIB) workstation (FEI Strata FIB 205). Prior to sectioning, the reaction layer was protected with gold (Au) and tungsten (W) coatings

1
2
3 deposited on each piece of bearing disc. All lamellae were prepared on the outer track of the bearing disc,
4 where the slip contribution was positive (Fig.1).
5

6 **3. Results and Discussions**

7 **3.1 TEM-Investigations**

8
9
10 TEM cross-section investigations were carried out on the outer tracks of all the bearing discs which were
11 tribologically tested. In the system with lubrication with low wear protection, an energy filtering TEM image
12 (Fig. 2) analysis showed that the reaction layer is mostly intact, but that the thickness varied strongly
13 between 0 - 100 nm. Bright field image analysis showed that the reaction layer apparently exhibited bubbles
14 inside. The electron transparent bubbles are surrounded by solid material. Analysis of high resolution TEM
15 micrographs proved that the solid reaction layer is formed by an amorphous iron oxide with embedded
16 nanocrystalline particles, which could be identified as Fe_2O_3 . EFTEM-analysis revealed that Fe and O are
17 the main constituents forming the solid reaction layer. Additional EDX analysis showed that small amounts of
18 several of the additive-elements, specifically K, Ca and S are present. The chemical composition and
19 thickness are in accordance with the results obtained by Evans et al. in investigations of antiwear (AW)
20 surface-layers formed under the presence of mineral oil with sulphur-phosphorus (S-P) additives [5].
21 Underneath the reaction layer, there is a fine crystalline plastic deformation zone with a thickness of ~ 400
22 nm.

23
24 In the system with lubrication with high wear and fatigue protection, a very thin continuous reaction layer with
25 a median thickness value of 6 nm is formed (Fig. 3). EFTEM-analysis verified that Fe and O are also the
26 main constituents forming the reaction layer of the system with lubrication with high wear and fatigue
27 protection. EDX analysis revealed the presence of very small amounts of the additive-elements S and P. An
28 analysis of high resolution TEM micrographs proved that the reaction layer is also formed by amorphous iron
29 oxide with embedded nanocrystalline Fe_2O_3 particles. In addition, the effects of the strong plastic
30 deformation on the existing microstructure are visible in a subsurface layer with 200 nm thickness. In this fine
31 crystalline layer, we also found a chromium accumulation, which can be explained by the abrasion of
32 chromium carbides which get to the surface near area during the sliding process.

33
34 Figure 4 shows a TEM – BF micrograph of the sample with lubrication with high wear but low fatigue
35 protection. The reaction layer of this tribological system is characterised by an increasing thickness with
36 increasing load. The layers formed at a load of 2300 MPa and at 3250 MPa have a median thickness value
37 of about 40 nm and 70 nm, respectively. Similar to the first tribological system based on mineral oil, the
38 reaction layer included electron transparent bubbles. HRTEM and analytical TEM investigations revealed
39 that the solid phase of the reaction layer consists mainly of crystalline calcium phosphate. On the top of the
40 calcium phosphate layer, an amorphous iron oxide layer (~ 4 nm) has been deposited. EDX maps also
41 indicated that metallic zinc accumulated at the interface between the reaction layer and the substrate. The
42 elemental maps also showed low density bubbles inside the reaction layer. Similar to the systems with
43 lubrication with high wear and fatigue protection, the thickness of the tribomutation layer is about 200 nm.

44
45 The thickness of the reaction layer based on mineral oil totally agrees with the result of Evans [4, 5],
46 although it is assumed that the additives are completely different. The thickness and morphology of the
47 reaction layer depend strongly on the type of the base oil, whereas the chemical composition changes with
48 functional group and impact of the additives. A detailed report on the TEM analysis will be published
49 elsewhere.

50 **3.2 EPMA**

51
52 Electron Probe Micro Analysis (EPMA) measurements were used to determine the oxygen coverage across
53 the whole diameter of the bearing disc (Fig. 5) and thus to obtain a direct measure of the thickness of the
54 reaction layer, assuming a known density. All investigated tribological systems are covered with a reaction
55 layer in the load carrying area. For the bearing discs tested with the lubricant with low wear protection and
56 the lubricant with high wear but low fatigue protection, the thickness of the oxygen coverage is independent
57 of the load carrying area. In contrast, the bearing disc tested with lubricant with high wear and fatigue
58 protection showed a variation of the thickness of the oxygen coverage in the load carrying area which
59 depended on the sliding conditions. In the sliding zone the oxygen coverage is lower than in the rolling zone.
60 Further EPMA-investigations proved iron oxide to be the main component for the system with lubrication with
low wear protection and high wear and fatigue protection being accompanied with small incidences of other
elements like Ca, P and Zn and P, S, respectively. The reaction layer of the system with lubrication with high

wear and low fatigue protection based on calcium phosphate and contained a small amount of additive elements of Zn, Mg and S.

The results clearly show the impact of the additives. The iron oxide layers are formed mostly independent of the functional group of the additives, but depended on the load carrying area. Whereas the reaction layer of the lubricant with high wear and low fatigue protection formed independent of the load carrying area. The ESMA results totally agree with the analytical TEM investigation and thus ascertain that the results are representative for the whole layer system.

3.3 AFM

Atomic force microscope (AFM) images revealed that substantial surface smoothing occurred during the reaction layer formation in large regions of the tribological systems. We measured the surface roughness between the manufactured scorings due to polishing of the bearing discs, because the asperity-asperity contact appeared only there. The mean surface roughness of the systems with lubrication with low wear protection (Fig. 6) and high wear but low fatigue protection (Fig. 7) amounts to about 6 nm. Both samples exhibit a nano ripple component at the surface. The ripple was interpreted by Scherge [13] as result of the locally and temporally random energy dissipation of the micro contacts. In the present study, the ripple was only found on the systems based on mineral oil.

For the system with high wear protection (Fig. 8), the mean surface roughness only amounts to about 2 nm and shows no indication for ripple. In comparison, a polished reference sample has a roughness of about 1.2 nm, and the surface roughness of an unpolished reference sample is 40 nm (Fig. 9).

The surface smoothing on the bearing with low wear is positive for the reliability of the nanoindentation investigations, where a smooth surface topography has a high influence on the quality of the measurements.

3.4 Nanoindentation

Test measurements on 100Cr6 (bearing steel) were carried out at a maximum load of 5000 μN with a three-sided pyramidal Cube Corner tip. The total included angle of this tip is 90° and the radius of curvature is 180 nm. The nanomechanical properties of the different tribological layers were investigated by indentations obtained by the load variation method using a maximum load of 5000 μN with a sharp Cube Corner indenter. Indentation with 150 μN and 20 μN were made with a Berkovich indenter (tip radius of curvature of 160 nm). These measurements reveal the properties of the sample in the as-received condition of the layers.

The obtained load–displacement curves were corrected and analysed according to Oliver-Pharr-method [15, 16] with the routines supplied in the software package IndentAnalyser (ASMEC).

Each analysis point or curve is obtained by averaging over at least 10 and a maximum of 50 indentations.

3.4.1 Indentation measurements with 5000 μN

All systems with lubricants with low wear protection, high wear and fatigue protection, high wear but low fatigue protection, and a reference sample, were analysed by indenting the surface in the load carrying area and by indenting in the middle of polished cross-sections (denoted by 'X'). A comparison of elastic modulus for all systems measured with the maximum load of 5000 μN , is shown in Fig. 10. The curve depicts elastic modulus versus displacement into the surface.

All samples but the system with lubrication with high wear but low fatigue protection exhibit higher hardness in the load carrying area than in the polished cross section areas (bulk material).

The system with lubricant with high wear and fatigue protection and the reference sample exhibit very similar micromechanical behaviour. The elastic modulus is higher in the load carrying areas than in the bulk material in cross sections. Due to the surface finish the elastic modulus of the untreated reference sample is higher than the treated samples. The systems with low wear and high wear but low fatigue protection the elastic modulus is similar in the load carrying area than in cross sections. The influence of measurement position is also clearly visible in the displacement into the surface. The percentage elastic recovery (%R) of this material is given by

$$\%R = [(h_{\max} - h_c) / h_{\max}] * 100,$$

where h_{\max} is the maximum indentation depth and h_c is the contact depth [15, IndentAnalyser]. The %R values for the load carrying area measurements of reference sample, bearing disc with lubrication with high wear and fatigue protection and high wear but low fatigue protection are in average 6.3 %. The range of the values is typical of the response for a ductile metal, 100Cr6, and there is no considerable elastic recovery of the indentation depth once the load has been removed. The percentage elastic recovery for the system with

1
2
3 lubrication with low wear protection is not significantly higher and amounts to 6.6 %. The %R values for the
4 measurements of the polished cross-sections vary between 4.5 % - 5.5 %. The elastic recovery values in the
5 load carrying areas are thus about 1 % higher than in the polished cross-section bulk materials.

6 The %R value, h_{\max} and h_c are related to the plastic / elastic behaviour of the material and therefore also to
7 the (H/E) ratio of the material [17].

8 Finally, all systems have in common that during the tribological conditions the plasticity changed. Further
9 measurements with the continuous stiffness technique (CSM-technique) [11,18] are planned in order to work
10 out the differences between the different tribological systems.

11 12 **3.4.2 Indentation measurements with 150 μ N**

13
14 For the investigation of the nanomechanical properties of the tribomutation layer (fine crystalline zone) and
15 the reaction layer a load of 150 μ N was chosen. All systems with lubricant with low wear protection, high
16 wear and fatigue protection, high wear but low fatigue protection, and a reference sample, were analysed in
17 the load carrying area.

18 The results show that the elastic modulus (Fig. 11) of the system with lubrication with high wear and fatigue
19 protection is comparable to the reference sample and the indentation moduli of the two systems with
20 lubrication with low wear and high wear but low fatigue protection are very similar (see Fig. 11). The elastic
21 modulus of the reference sample and the sample with lubrication with high wear and fatigue protection,
22 determined at a load of 150 μ N, was also similar to the one determined at a load of 5000 μ N. The ultra thin
23 reaction layer does not seem to affect the elastic modulus. However, the hardness value of 14 GPa of both
24 systems is significantly higher than the hardness of the bulk material to 8 GPa (Fig. 12). By comparison to
25 the reference sample, we conclude that this is a result of work hardening. The planned CSM measurements
26 should clearly indicate the presence of work hardening for all tribological systems investigated.

27 The measurement data collected on the systems with lubrication with low wear and low fatigue protection,
28 respectively, reflected the thickness variation of the reaction layer. From 50 measurements on system with
29 lubrication with low wear protection 40 measurements revealed the properties of the tribomutation layer. At
30 the system with lubrication with low fatigue protection 30 of the 50 measurements reflected the properties of
31 the tribomutation layer. The indentation modulus (Fig. 11) of the systems with lubrication with low wear and
32 high wear but low fatigue protection is comparatively low and only reaches 150 GPa. The indentation
33 modulus is a compound modulus of reaction layer and tribomutation layer. The additional low hardness
34 values (Fig. 12) indicated a low resistance to plastic deformation of the reaction layer.

35 36 **3.4.3 Indentation measurements with 20 μ N**

37
38 For the investigation of the nanomechanical properties of the reaction layer alone a load of 20 μ N was
39 chosen. In order to determine elastic modulus, it is necessary to acquire reproducible entirely elastic load-
40 displacement curves. From these curves, elastic moduli can be calculated by elastic fit to the entire elastic
41 load-displacement curves (Software package: IndentAnalyser). However, the elastic fit is only possible if the
42 elastic modulus of the tribomutation layer is known.

43 In our present investigations, only the system with lubrication with high wear and fatigue protection and a
44 reference sample were examined over the whole elastic range.

45 The result is that the reference sample has a Young's modulus with a value of 177 GPa, which is in the
46 range of the previous measurements on the systems with lubrication with low wear and high wear but low
47 fatigue protection with a load at 150 μ N. Therefore, it is a compound modulus, which may include
48 contributions by deposited contamination. However, the compound modulus resulting of the amorphous
49 oxide layer and the underlying fine crystalline zone of the sample with lubrication with high wear and fatigue
50 protection has a value \sim 130 GPa. By using the initially described elastic fit method, the amorphous oxide
51 layer has a rather low Young's modulus with 46 GPa calculated with Poisson's ratio estimated to 0.27, which
52 is also used for the matrix. The correct measurement of the Poisson's ratio is difficult. Therefore it is common
53 to assume for oxides the same value, or a little bit lower by 0.05-0.1. If the Poisson's ratio decreases by
54 about 0.1 the Young's Modulus increases about 10 GPa. For comparison fused silica has a Young's
55 modulus of 72 GPa.

56 Fig. 13 shows a comparison of the fully elastic experimental load-displacement data of the reference sample
57 as well as the sample with lubrication with high wear and fatigue protection with the simulation for the
58 reference sample and a one layer system under assumption of a spherical indenter (indenter radius 160 nm).
59 The simulation was performed with the software package Elastica (ASMEC).

60
As a final remark, we want to point out that the nanoindentation measurements were performed rather
closely to the upper and lower load limit of the Triboscope, respectively and due to the small load range 0 -

9500 μN the indenter tips were changed. Therefore, it is mandatory to get some independent measure, to what extent these load limits the accuracy of the measurements. Therefore we plan to perform additional nanoindentation measurements with different methods and instruments.

3.4.4 TEM-studies on nanoindents cross-sectioned with the FIB-technique

For understanding the functionality of the very thin reaction layers formed by the lubricant with high wear and fatigue protection and the underlying tribomutation layer, TEM-studies were conducted on nanoindents cross-sectioned with FIB-technique. For comparison the same experiments were also performed on a polished reference sample. For these investigations, the samples were covered with arrays of indents and FIB-lamellae were cut containing several indents.

For the investigated indents in both systems, the load-depth curves recorded with a maximum load of 5000 μN were merely identical. The resulting hardness values were identical in both systems with an average value of 8.5 GPa. Furthermore, the Young's modulus also shows little difference for both systems with a value of 224 GPa for the polished reference sample and 208 GPa for the system obtained with lubrication with high wear and fatigue protection.

In overview images, the indents show an identical morphology. Both samples have pile-ups at the edge of the indent. The system obtained with the lubricant with high wear and fatigue protection exhibits a bright layer on the surface above the fine crystalline tribomutation layer (Fig. 14). This indicates that even though the reaction layer and the fine crystalline zone are penetrated by the indents, the reaction layer remains intact during the indentation, see arrows on Figure 14.

The polished reference sample (Fig. 15) has of course no reaction layer and no fine crystalline zone and the surface is really smooth.

At higher magnification, differences between the indents in the different systems are evident. Figure 14 shows a well-defined indent in the system with lubrication with high wear and fatigue protection, whereas the polished reference sample shows a corrugated indent (Fig. 15). This can be explained by the fact, that all three indents in the FIB lamella of the polished reference sample showed adhesion effects of the substrate material to the indenter tip during the unloading process, see arrows on Figure 15.

As a consequence, the polished reference sample must have formed pile-ups along the glide planes.

The result of our investigation makes it possible to deduce the behaviour of the system with lubrication with high wear and fatigue protection, when subjected to particle wear like interpenetrating chromium carbides which have the same dimensions as the indent. The fine crystalline microstructure of the tribomutation layer is able to accommodate to the disturbance and to adsorb the energy of the plastic deformation.

4 Conclusions

In the present investigations, microstructure, chemical composition and mechanical properties (hardness, Young's modulus and indentation modulus, respectively) of tribological systems with three different types of lubricants were analysed and the results were put in relation to each other. In a standardised FE-8 test rig, a model type of 100Cr6 cylinder roller bearings was emerged in a bath of lubricants with low wear protection, high wear and fatigue protection as well as high wear but low fatigue protection. The experimental test were run at 80 °C under varying load and speed conditions, which favour sliding in the boundary lubrication regime. Based on the obtained results, the following main conclusions can be drawn from the present study:

- i. The formation and the morphology of the reaction layer depended strongly on the base oil type used for lubrication. Ester-based oils (Type PAO/E) promote the formation of single, iron oxide-based ultra thin reaction layers with an average thickness of 6 nm. The corresponding lubricant delivered high wear and fatigue protection, in which the properties of the ultra thin reaction layer seem to play an important role. Mineral oil based lubricants cause the formation of much thicker reaction layers with a complex morphology. Whereas the lubricant with low wear protection stimulated the formation of a discontinuous, iron oxide reaction layer with strongly varying thickness, the lubricant with high wear but low fatigue protection led to the formation of calcium phosphate-based layer with a much more uniform thickness. In the latter case, the layer thickness showed a significant dependence on the applied load level. It should be mentioned that all the lubricants contained sulphur and phosphorus additives and the lubricants delivering high wear protection were of very similar viscosity.
- ii. In the matrix underneath the reaction layer, a tribomutation layer forms which is characterised by a fine crystalline defect – rich microstructure caused by the heavy plastic deformation. The thickness of the tribomutation layer depends on the amount of wear protection provided by the lubricant and is

1
2
3 in the order of 200 nm in the case of high wear protection and of about 400 nm for lubricants with low
4 wear protection.
5

- 6 iii. The results of our studies present clear evidence that the combined action of the reaction layer and
7 the tribomutation layer controls the tribological properties of the systems investigated. In particular
8 the TEM studies of cross-sectioned nanoindentations revealed that the reaction layer is capable of
9 providing sufficient adhesion protection even in the case of severe plastic deformation and in the
10 absence of any lubricants. It is also remarkable that in particular the ultra thin reaction layer seems
11 to most perfectly serve for this purpose. Under non adhesive conditions, the severe plastic
12 deformation under the applied frictional sliding conditions lead to a substantial surface smoothing
13 and hardening effect in the load carrying areas. As verified by our TEM and nanoindenter
14 investigations, the latter can directly be explained by the Hall – Petch effect in the fine crystalline
15 tribomutation layer.

16 As a final remark, it should be noted that under the action of the lubricants with high wear protection,
17 the reaction layer / tribomutation layer system must be rapidly self-reproducing, given that under the
18 applied tribological loads it is impossible to avoid strong local abrasion.
19
20

21 Acknowledgement

22
23 The authors are grateful to the Deutsche Forschungsgemeinschaft (DFG) for the financial support [GO
24 684/8-3 and MA 1280/22-1] and the European Commission of Nanobeams Network of Excellence [FP6-
25 500440-2]
26

27 References

- 28
29 [1] Uetz H., Foehl, J., Sommer K., Antriebstechnik 28 (1989) 10, 57-62
30
31 [2] Meyer K., Tribologie und Schmierungstechnik 5,
32
33 [3] 1985 Meyer K., Kloß H., Reibung und Verschleiß geschmierter Reibsysteme, Expert Verlag, 1993
34
35 [4] EVANS R. D., More K. L., Darragh C.V., and Nixon H. P., Tribology Transactions, 47: 430-439, 2004
36
37 [5] EVANS R. D., More K. L., Darragh C.V., and Nixon H. P., Tribology Transaction, 48: 299-307, 2005
38
39 [6] Loos J., PhD-thesis, RWTH Aachen, Germany, 2001
40
41 [7] DIN EN ISO 51819-T
42
43 [8] Gold P. W., Tribology lecture 2003
44
45 [9] DIN 51819
46
47 [10] Karduck, P., Ammann, N., Microbeam Analysis, 1990:21
48
49 [11] Fischer-Cripps A. C., Nanoindentation, Springer-Verlag, 2.Auflage 2004
50
51 [12] REICHEL M., WEIRICH TH., RICHTER S., ARETZ A., MAYER J., WOLF TH., KLAAS H., LOOS J., GOLD P. W.,
52 Trib. und Schmierungstechnik 02/05, 18-23
53
54 [13] Scherge, M., Chakhvorostov, D., Pöhlmann, K. Trib. und Schmierungstechnik, 3/03, 5-9
55
56 [14] Chudoba, T., Richter, F.: Surface and Coatings Technology 148 (2001) 191-198
57
58 [15] Oliver, W. C. and Pharr, G. M., J. Mater. Res., Vol. 7, No6, June 1992
59
60 [16] Pharr, G. M, Oliver, W. C. and Brotzen, F. R J. Mater. Res., Vol. 7, No. 3, Mar 1992
[17] Hainsworth, S. V. and Page, T. F., Nondestructive Testing and Evaluation, Vol.4, pp.275-298, 2001

1
2
3
4
5
6
7
8
9
10
11
12
13
14
15
16
17
18
19
20
21
22
23
24
25
26
27
28
29
30
31
32
33
34
35
36
37
38
39
40
41
42
43
44
45
46
47
48
49
50
51
52
53
54
55
56
57
58
59
60

[18] www.mtsnano.com/pdf/Nano_CSM.pdf

For Peer Review Only

Oil classification	load level	conditions	contact pressure	breakdown
low wear protection	1	30 kN, 15 rollers	1150 MPa	Yes, m > 10 mg
	2	50 kN, 15 rollers	1490 MPa	
	3	80 kN, 15 rollers (FE8 Standard)	1890 MPa	
high wear and fatigue protection	4	80 kN, 10 rollers	2300 MPa	No, m < 10 mg
high wear but low fatigue protection	5	80 kN, 5 rollers	3250 MPa	No, m < 10 mg

1
2
3
4
5
6
7
8
9
10
11
12
13
14
15
16
17
18
19
20
21
22
23
24
25
26
27
28
29
30
31
32
33
34
35
36
37
38
39
40
41
42
43
44
45
46
47
48
49
50
51
52
53
54
55
56
57
58
59
60

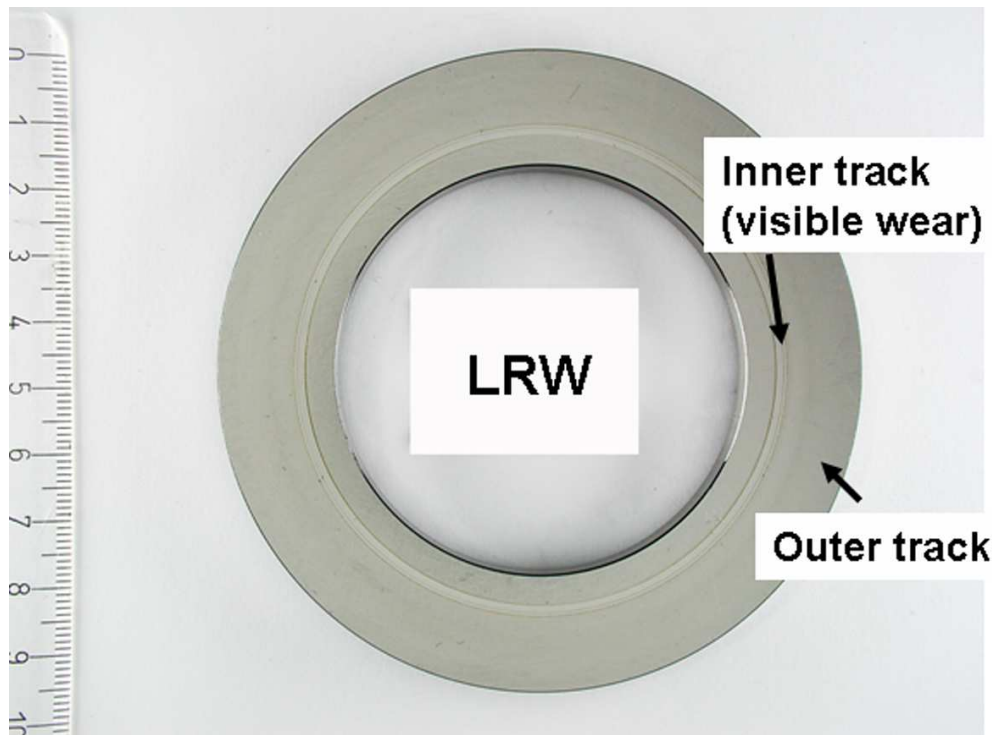


Figure 1: Photograph of bearing disc treated with lubricant with low wear protection. Inner track shows impact of macroscopic wear.

99x72mm (300 x 300 DPI)

Pre-proof Only

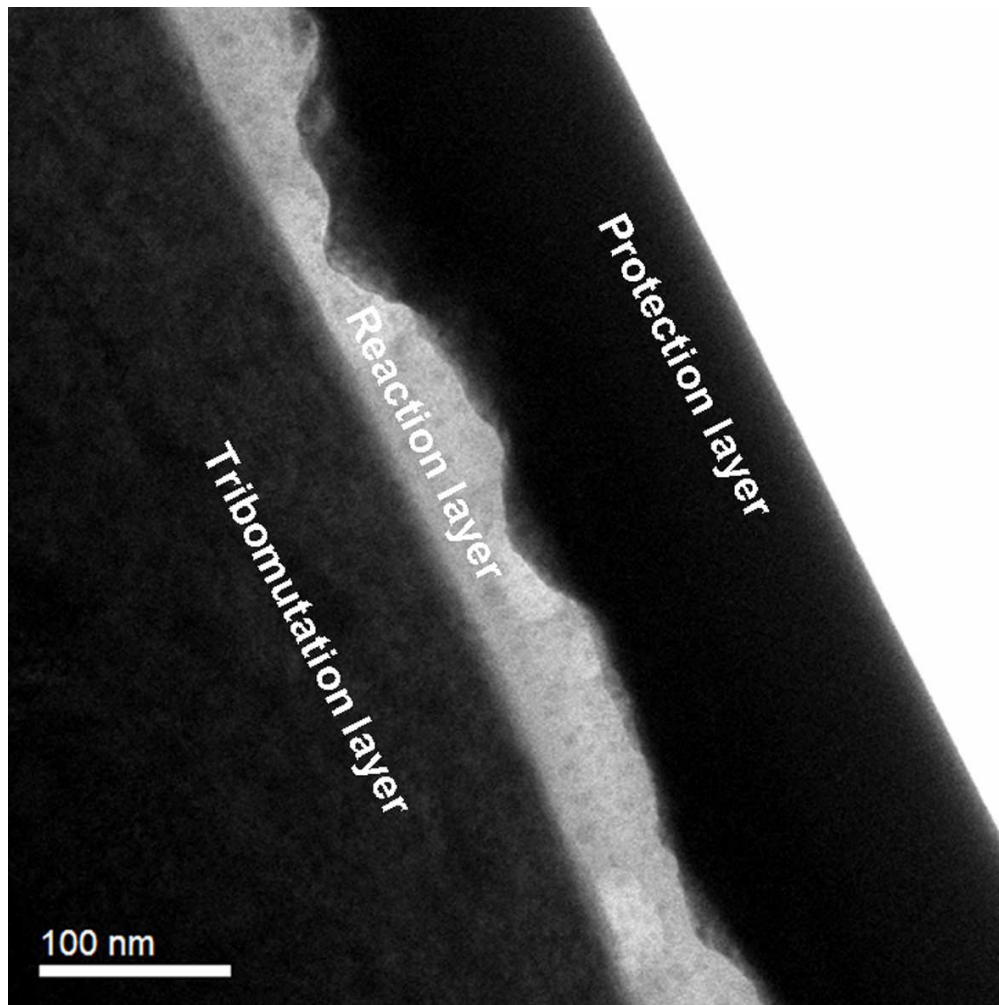


Figure 2: Energy filtering TEM (EFTEM) image of the reaction layer formed on the sample w with low wear protection lubrication.

99x99mm (300 x 300 DPI)



1
2
3
4
5
6
7
8
9
10
11
12
13
14
15
16
17
18
19
20
21
22
23
24
25
26
27
28
29
30
31
32
33
34
35
36
37
38
39
40
41
42
43
44
45
46
47
48
49
50
51
52
53
54
55
56
57
58
59
60

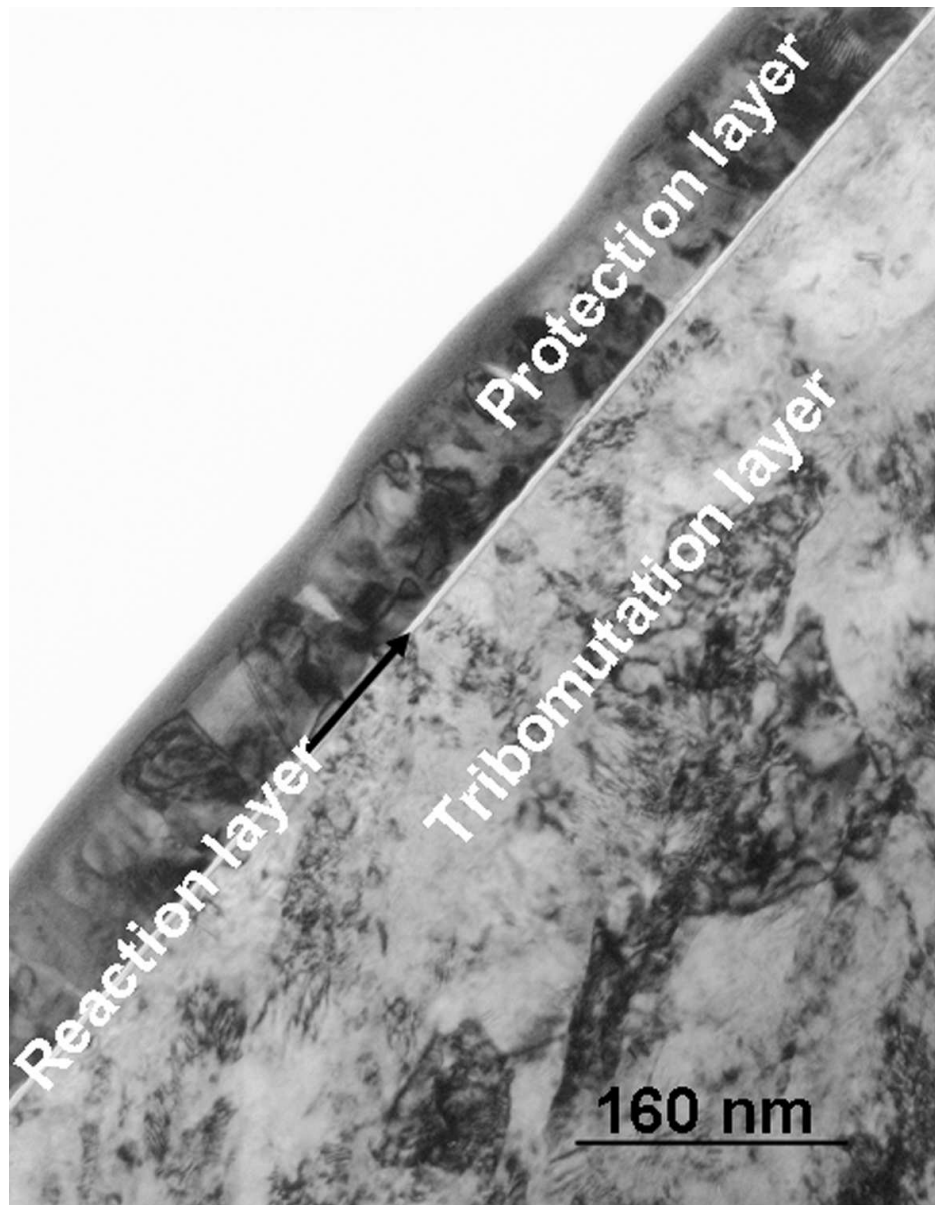


Figure 3: TEM – BF micrograph of the sample with lubricant with high wear and fatigue protection. The arrow marks the ultra thin reaction layer.

99x128mm (300 x 300 DPI)

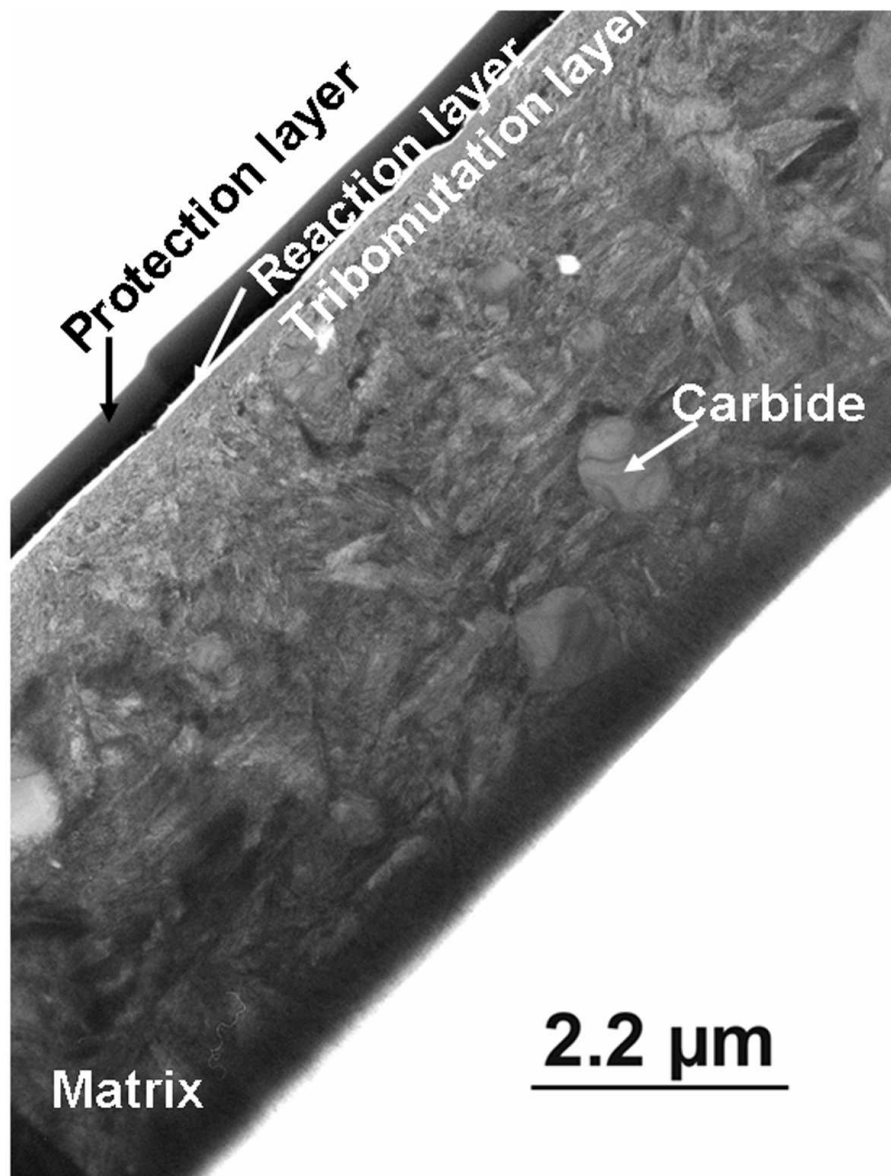


Figure 4: TEM – BF micrograph of the sample with lubricant with high wear but low fatigue protection.
99x133mm (300 x 300 DPI)

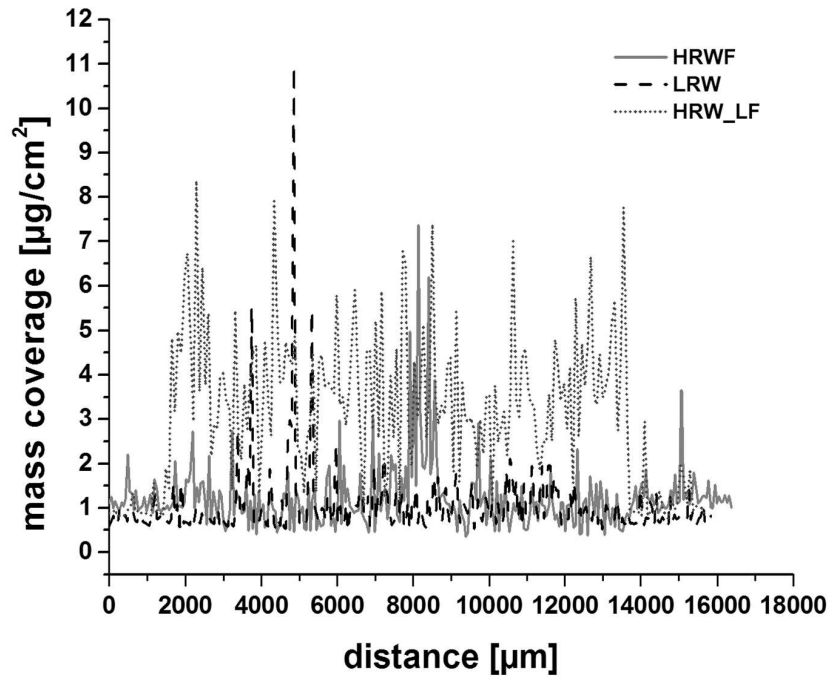


Figure 5: EPMA linescans, oxygen mass coverage versus distance on the bearing disc. Measurement was performed from the inner side (zero) to the outer side of the bearing disc (scanned distance 16000 μm).

Abbreviations are:

LRW: Low references wear protection [1150 MPa 8 h (mineral oil, Ca-P-S additives)]

HRWF: High references wear and fatigue protection [2300 MPa 80 h (PAO/E, P-S additives)]

HRW_LF: High references wear but low fatigue protection [2300 MPa 80 h (mineral oil, Ca-Zn-P-S additives)].

279x215mm (300 x 300 DPI)

1
2
3
4
5
6
7
8
9
10
11
12
13
14
15
16
17
18
19
20
21
22
23
24
25
26
27
28
29
30
31
32
33
34
35
36
37
38
39
40
41
42
43
44
45
46
47
48
49
50
51
52
53
54
55
56
57
58
59
60

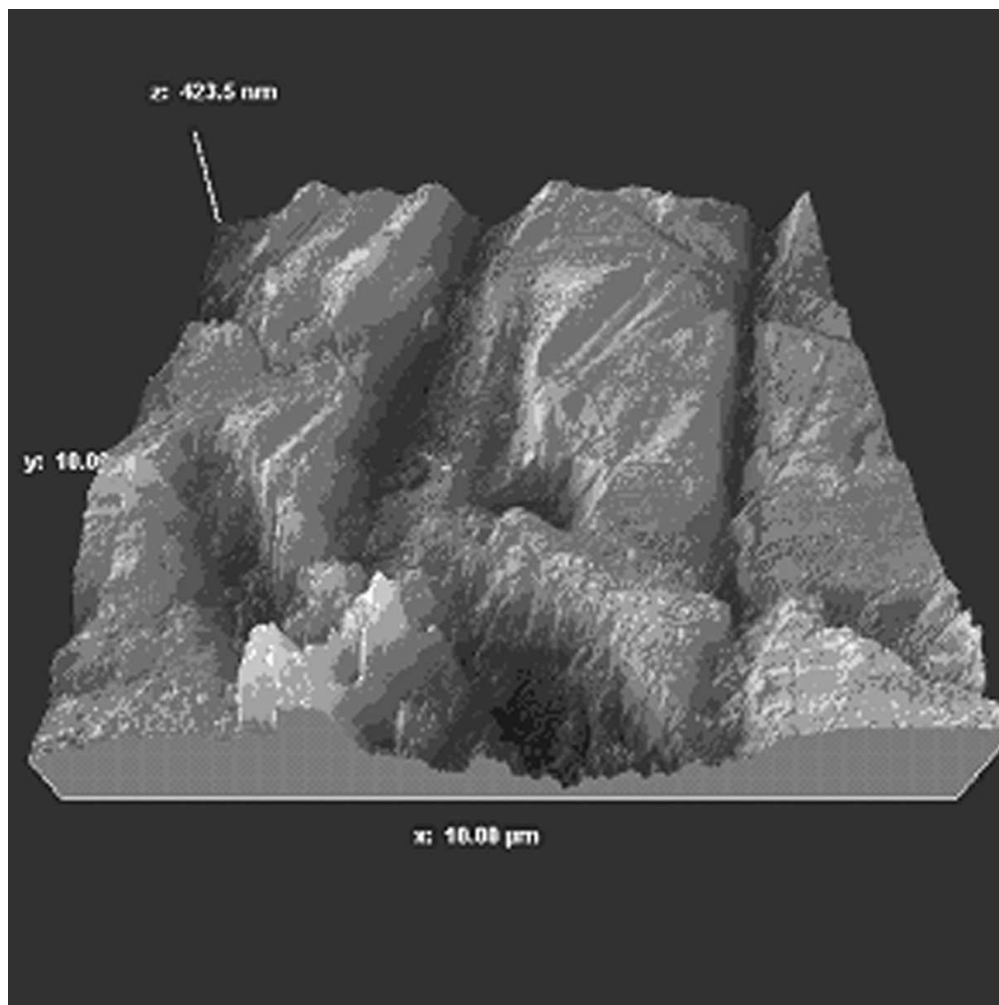


Figure 6: AFM topographic image from the surface of the system with lubricant with low wear protection.

102x102mm (300 x 300 DPI)



1
2
3
4
5
6
7
8
9
10
11
12
13
14
15
16
17
18
19
20
21
22
23
24
25
26
27
28
29
30
31
32
33
34
35
36
37
38
39
40
41
42
43
44
45
46
47
48
49
50
51
52
53
54
55
56
57
58
59
60

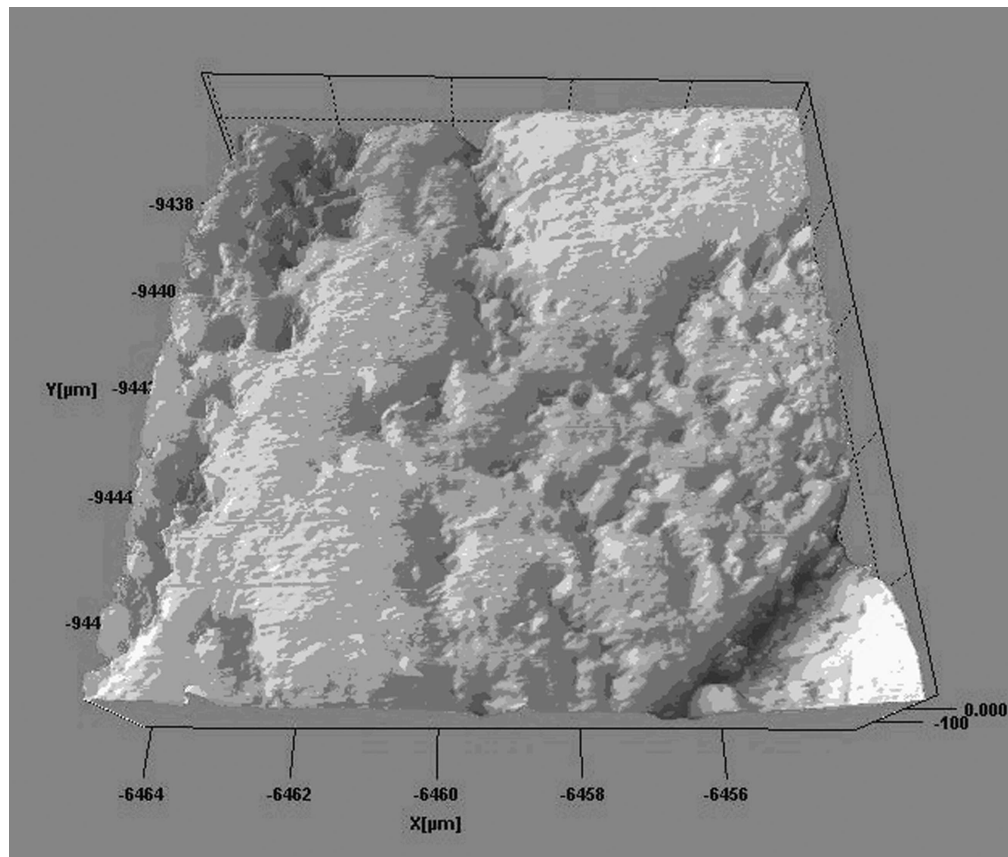


Figure 7: AFM topographic image from the surface of the system with lubricant with high wear but low fatigue protection. 219x186mm (300 x 300 DPI)

Only

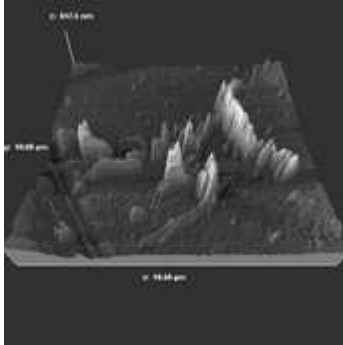


Figure 8: AFM topographic image from the surface of the system with lubricant with high wear protection.
14x14mm (300 x 300 DPI)

Peer Review Only

1
2
3
4
5
6
7
8
9
10
11
12
13
14
15
16
17
18
19
20
21
22
23
24
25
26
27
28
29
30
31
32
33
34
35
36
37
38
39
40
41
42
43
44
45
46
47
48
49
50
51
52
53
54
55
56
57
58
59
60

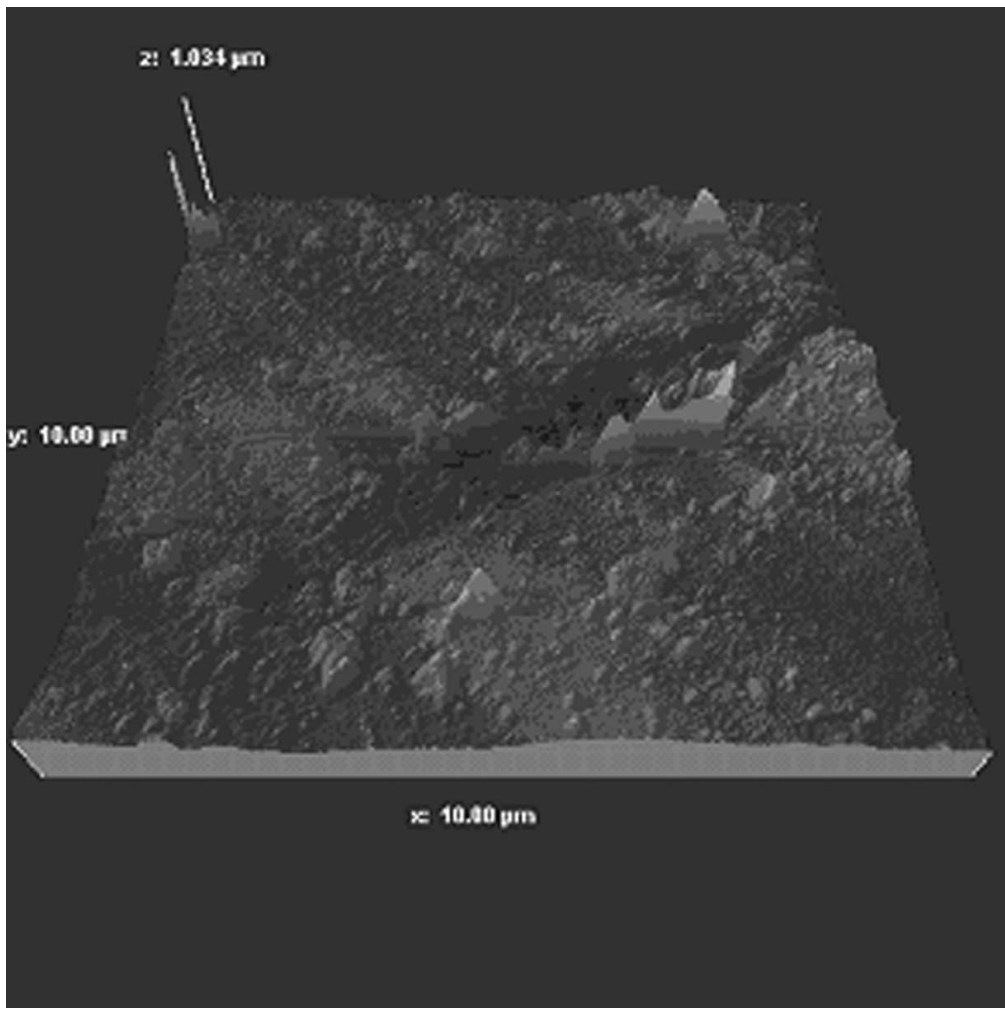


Figure 9: AFM topographic image from the surface of an untreated reference sample.

102x102mm (300 x 300 DPI)

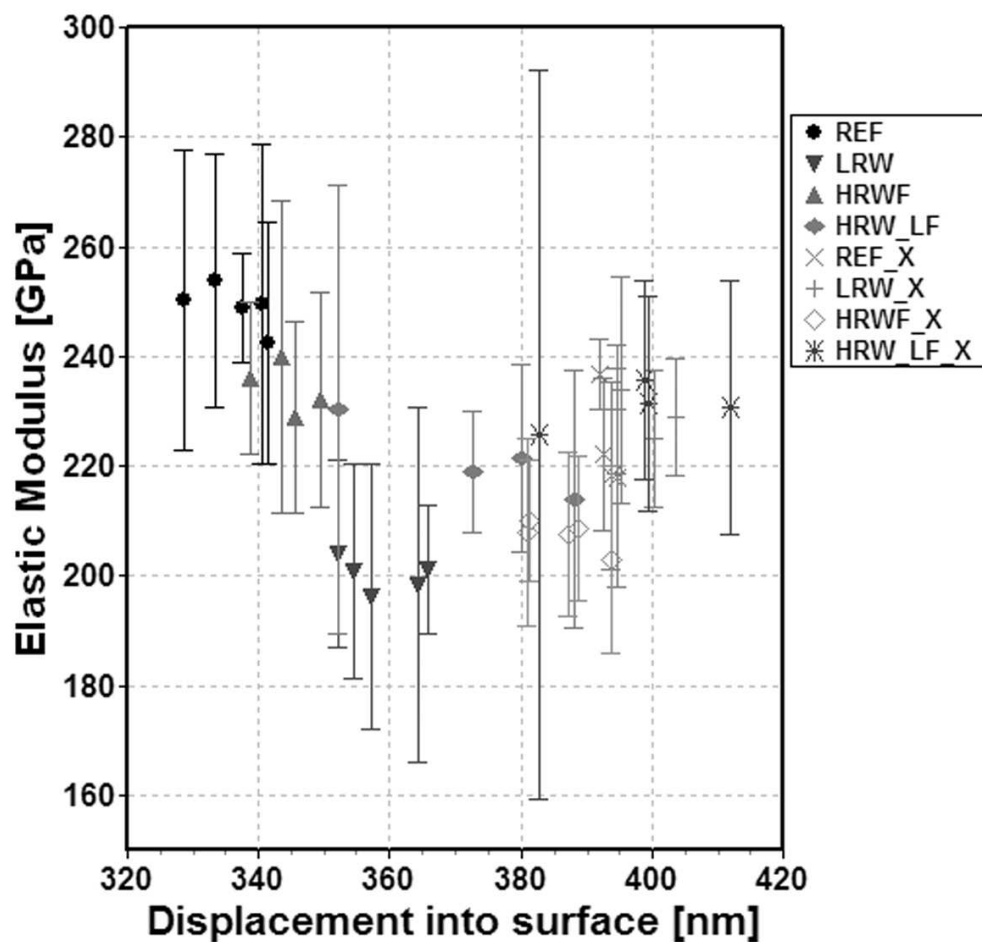


Figure 10: Comparison elastic modulus measured at a maximum load of 5000 μN with Cube Corner indenter. Abbreviations and experimental conditions are:

REF: Reference sample

LRW: Low references wear protection [1150 MPa 8 h (mineral oil, Ca-P-S additives)],

HRWF: High references wear and fatigue protection [2300 MPa 80 h (PAO/E, P-S additives)],

HRW_LF: High references wear but low fatigue protection [2300 MPa 80 h (mineral oil, Ca-Zn-P-S additives)],

Additional 'X': cross section investigations in the middle of the surface (bulk material).

99x95mm (300 x 300 DPI)

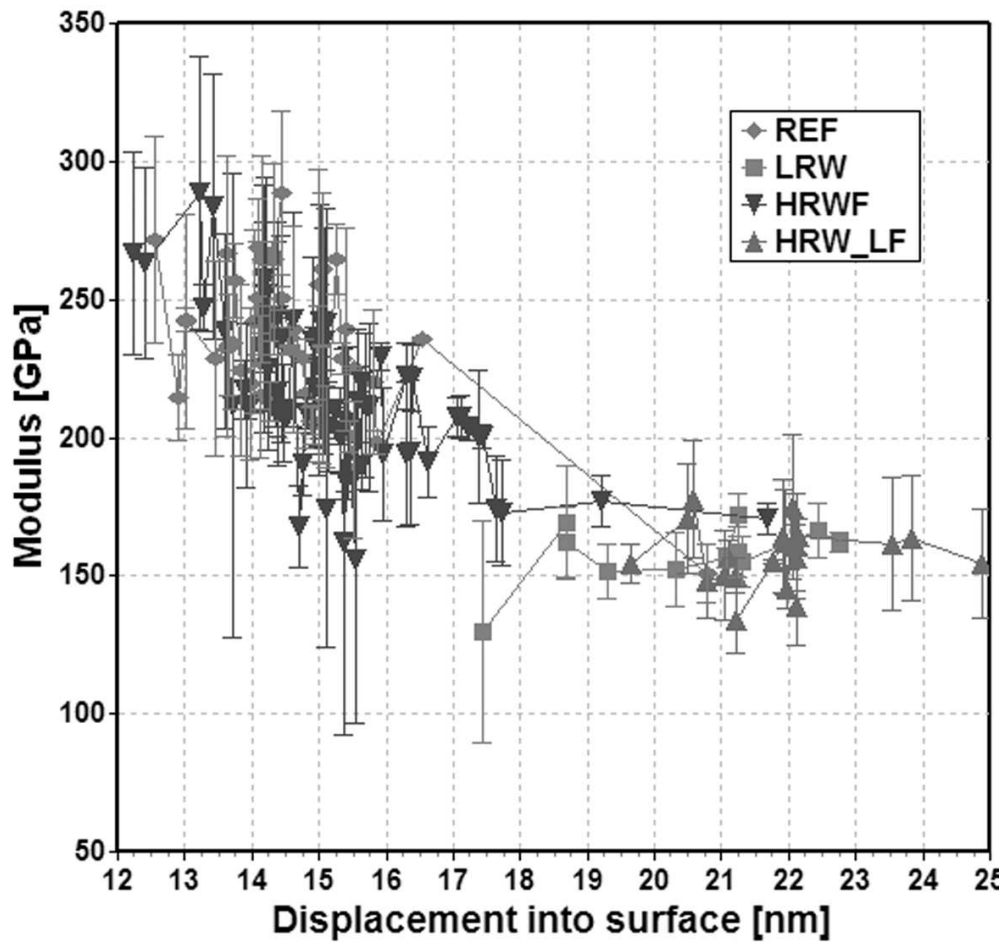


Figure 11: Comparison of elastic modulus measured at a maximum load of 150 μN with Berkovich indenter. Abbreviations and experimental conditions see Figure 10.
99x95mm (300 x 300 DPI)

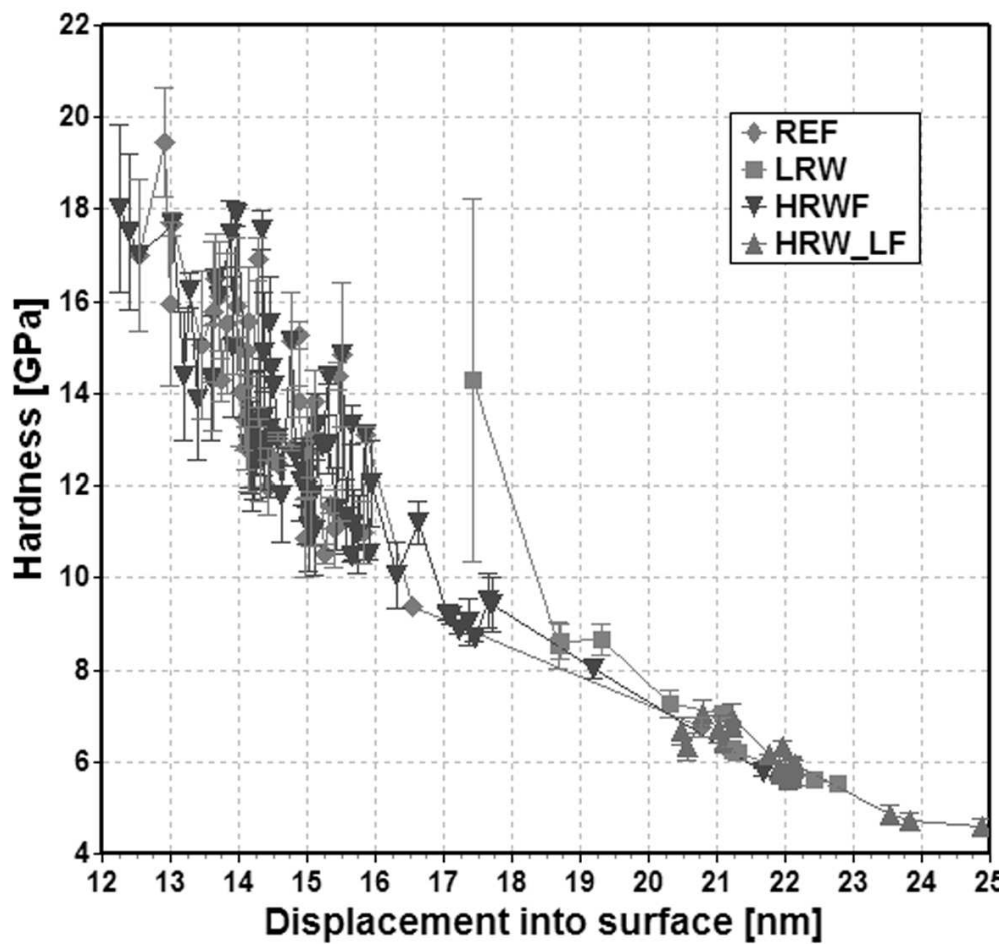


Figure 12: Comparison of hardness measured at a maximum load of 150 μN with Berkovich indenter. Abbreviations and experimental conditions see Figure 10.
99x95mm (300 x 300 DPI)

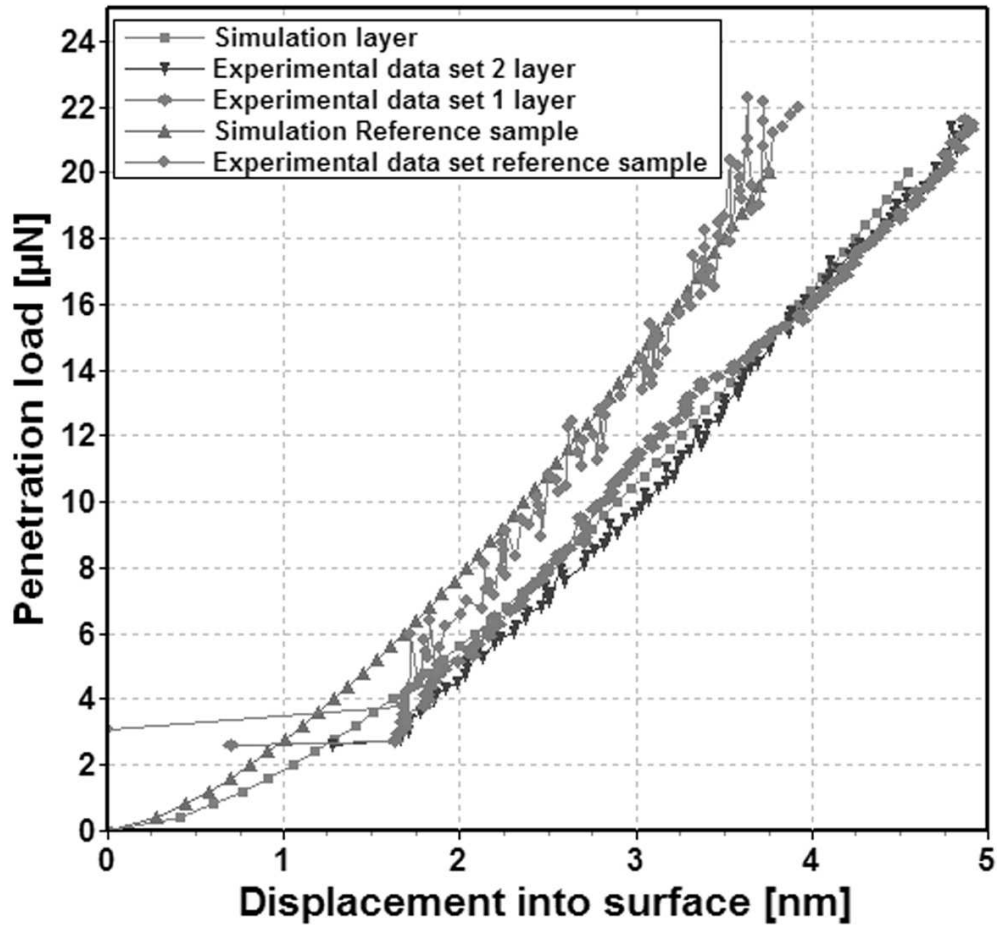


Figure 13: Comparison of experimental data with simulation with a maximum load of 20 µN. The simulations were performed by Elastica (ASMEC).

99x95mm (300 x 300 DPI)



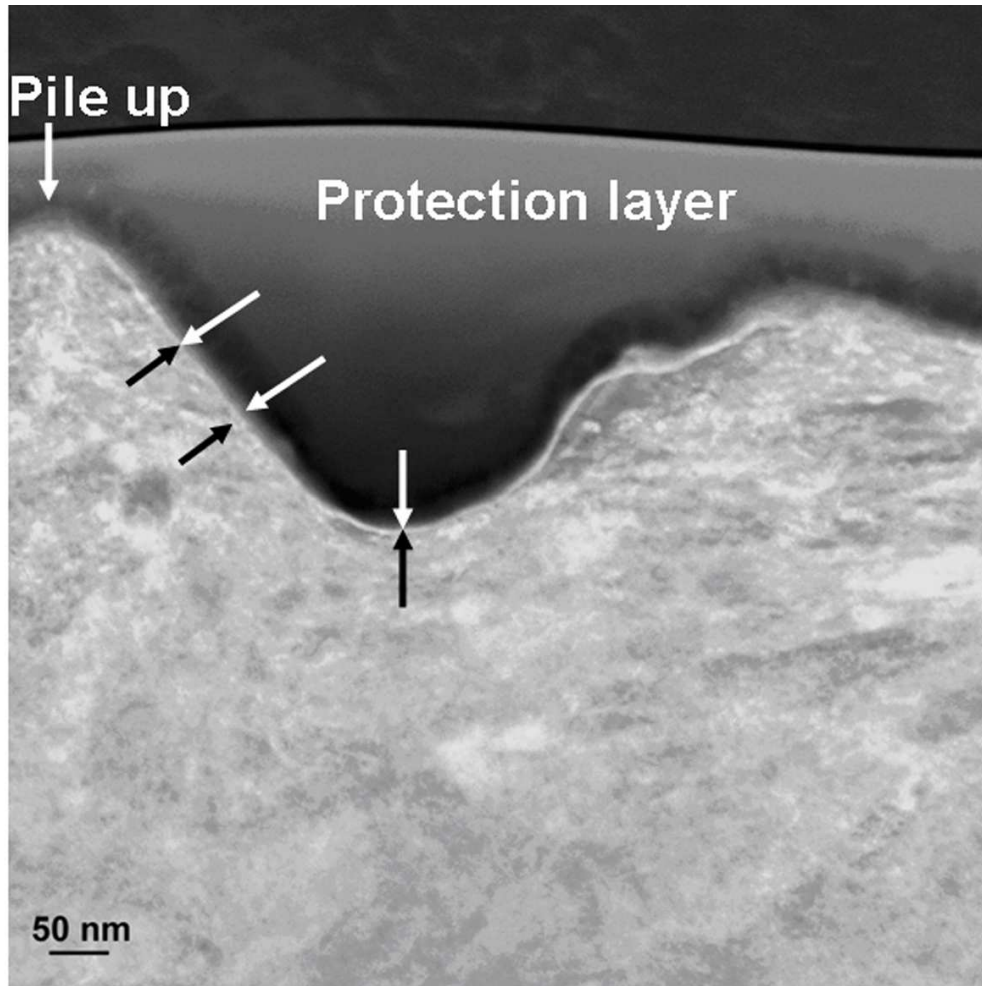


Figure 14: STEM-DF image at higher magnification of a nanoindent in the system formed with lubrication with high wear and fatigue protection. The region of the ultra thin reaction layer is marked by arrows.

99x98mm (300 x 300 DPI)



1
2
3
4
5
6
7
8
9
10
11
12
13
14
15
16
17
18
19
20
21
22
23
24
25
26
27
28
29
30
31
32
33
34
35
36
37
38
39
40
41
42
43
44
45
46
47
48
49
50
51
52
53
54
55
56
57
58
59
60

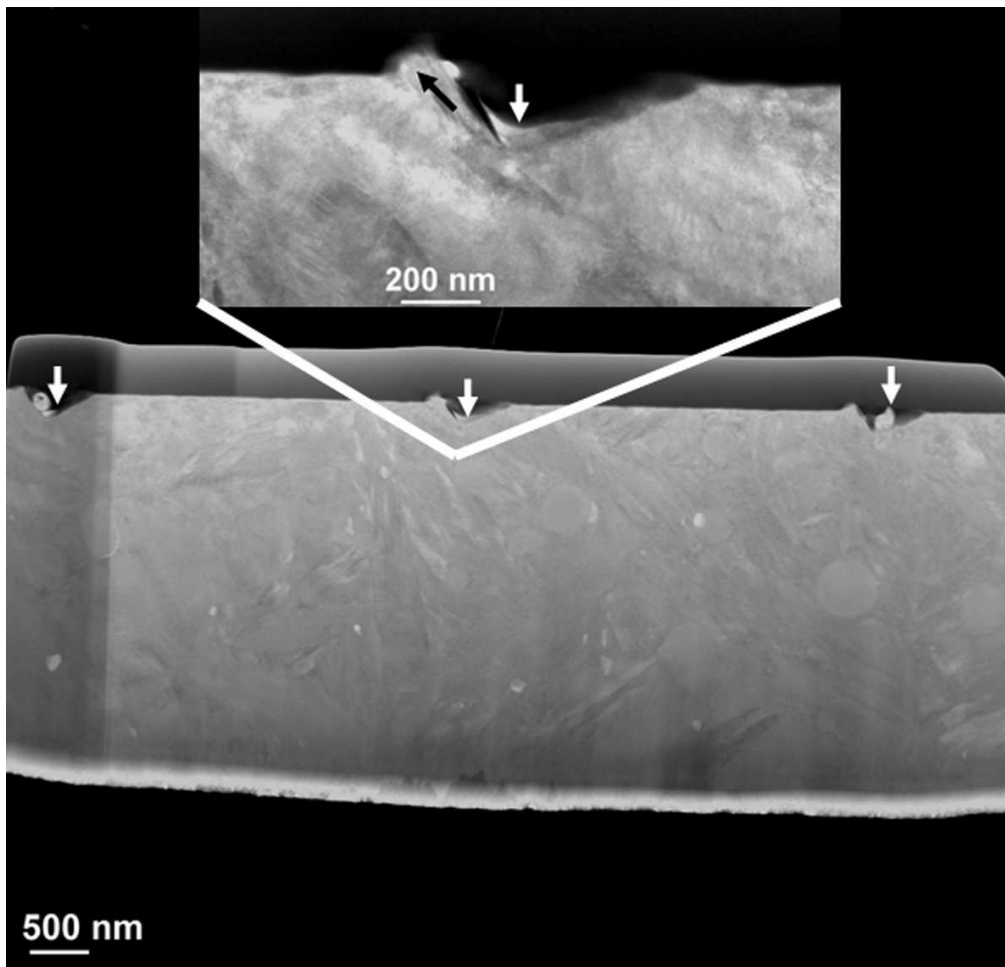


Figure 15: STEM - DF- micrographs of the nanoindentations in an untreated, polished reference sample. White arrows mark matrix material inside the indents and the black arrow mark the pile up formed by slide plane.
99x96mm (300 x 300 DPI)

